A

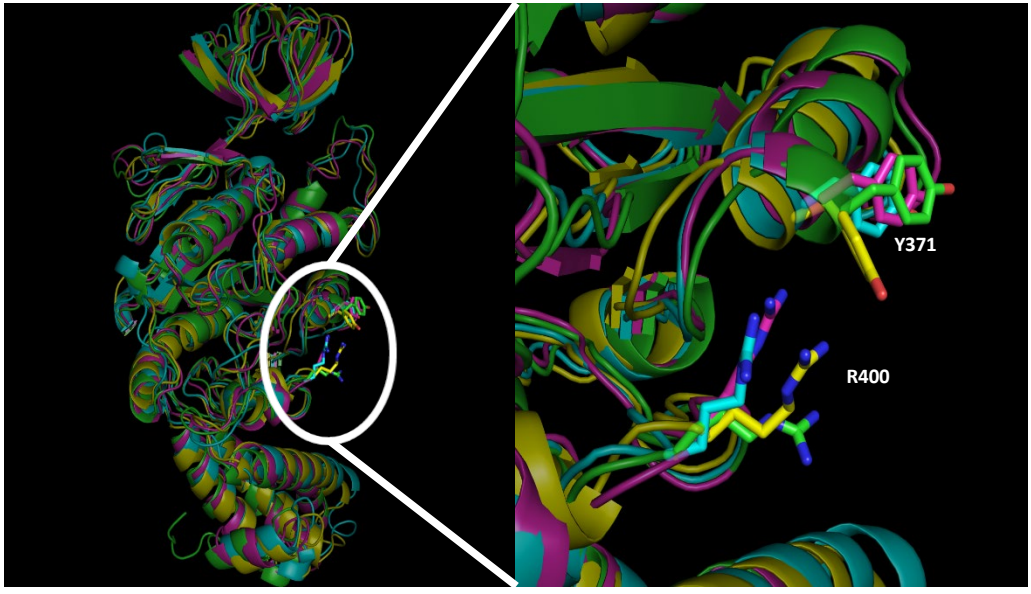

B

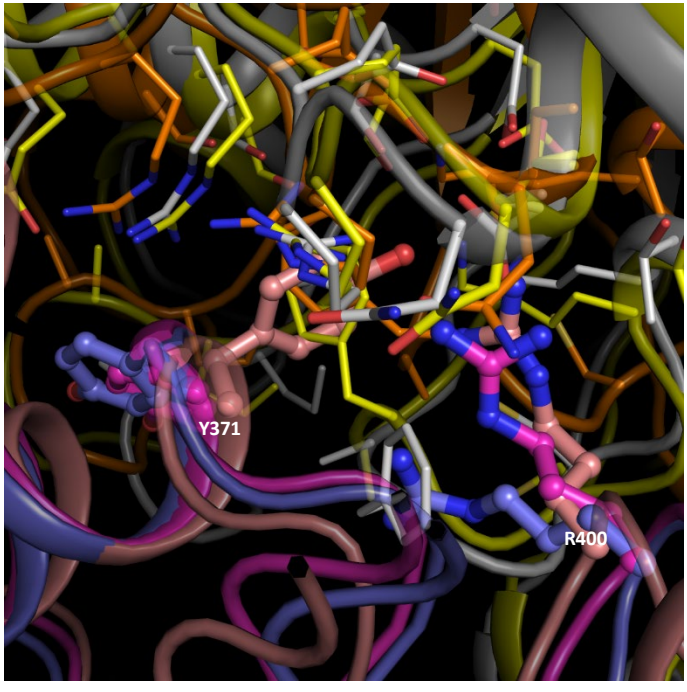

S Figure 1

A

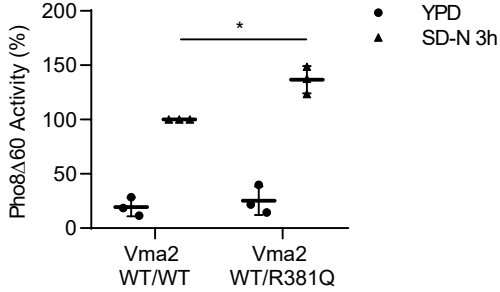
200
150
100
50
0
Pho8Δ60 Activity (%)
*
YPD
SD-N 3h
Vma2
WT/WT
Vma2
WT/R381Q

B

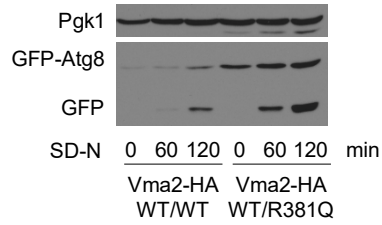
Pgk1
GFP-Atg8
GFP
SD-N
0 60 120 0 60 120 min
Vma2-HA
WT/WT
Vma2-HA
WT/R381Q

S Figure 2

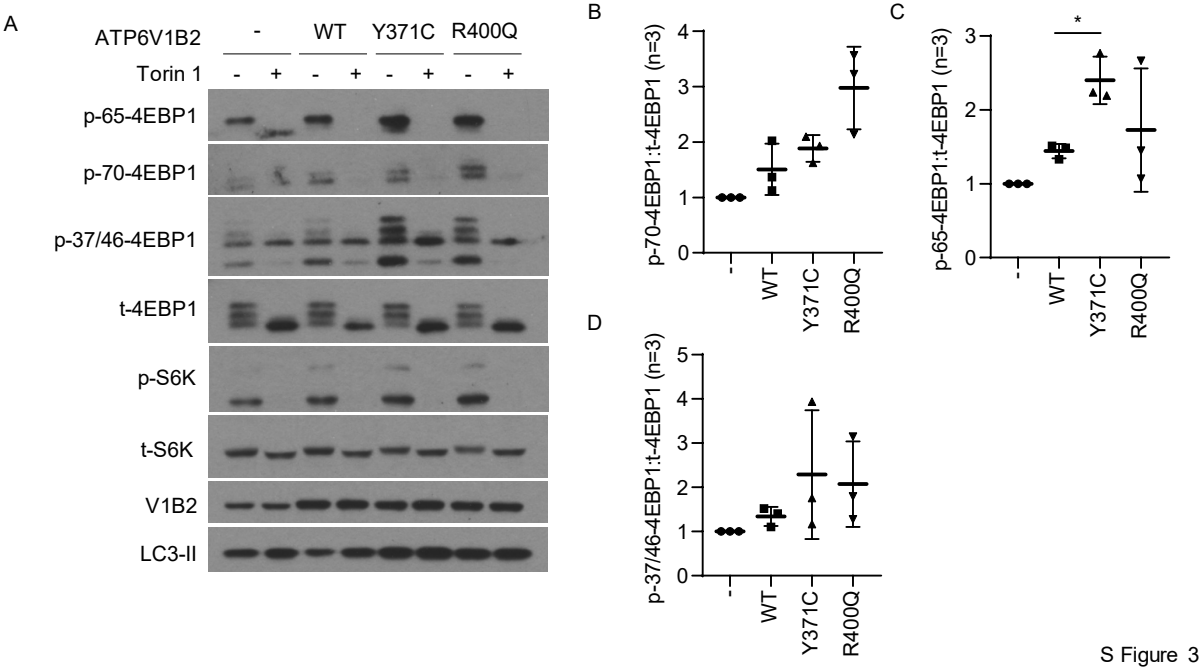
A
ATP6V1B2
-
WT
Y371C
R400Q
Torin 1
- + - + - + - +
p-65-4EBP1
p-70-4EBP1
p-37/46-4EBP1
t-4EBP1
p-S6K
t-S6K
V1B2
LC3-II
B
p-70-4EBP1:t-4EBP1 (n=3)
0
1
2
3
4
-
WT
Y371C
R400Q
C
p-65-4EBP1:t-4EBP1 (n=3)
*
0
1
2
3
-
WT
Y371C
R400Q
D
p-37/46-4EBP1:t-4EBP1 (n=3)
0
1
2
3
4
5
-
WT
Y371C
R400Q

S Figure 3

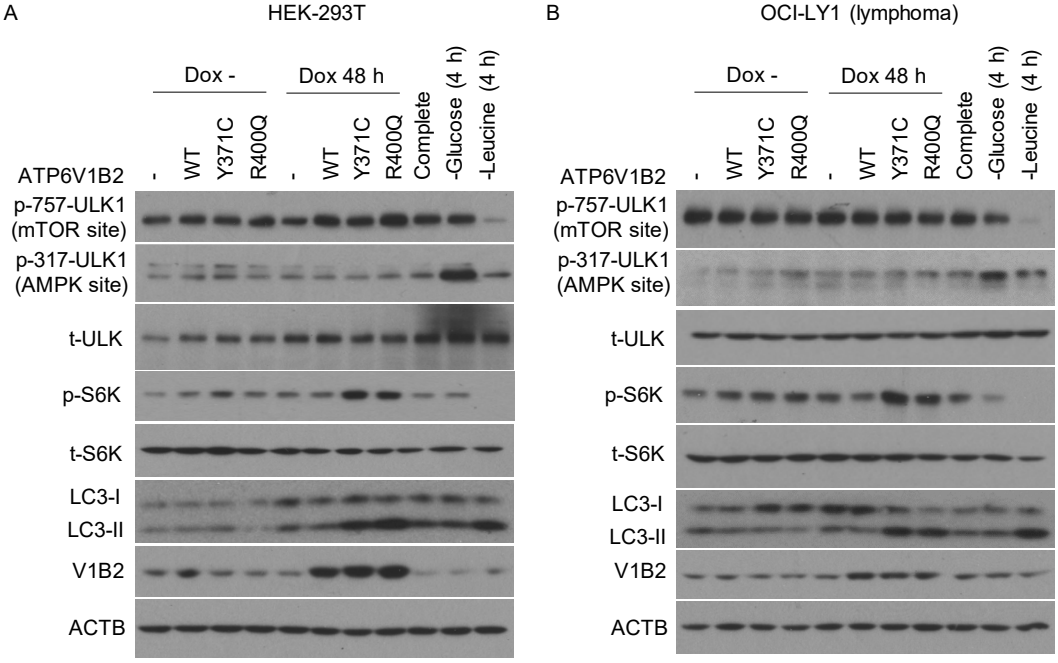
A
HEK-293T
Dox -
Dox 48 h
-
WT
Y371C
R400Q
-
WT
Y371C
R400Q
Complete
-Glucose (4 h)
-Leucine (4 h)
ATP6V1B2
p-757-ULK1 (mTOR site)
p-317-ULK1 (AMPK site)
t-ULK
p-S6K
t-S6K
LC3-I
LC3-II
V1B2
ACTB
B
OCI-LY1 (lymphoma)
Dox -
Dox 48 h
-
WT
Y371C
R400Q
-
WT
Y371C
R400Q
Complete
-Glucose (4 h)
-Leucine (4 h)
ATP6V1B2
p-757-ULK1 (mTOR site)
p-317-ULK1 (AMPK site)
t-ULK
p-S6K
t-S6K
LC3-I
LC3-II
V1B2
ACTB

S Figure 4

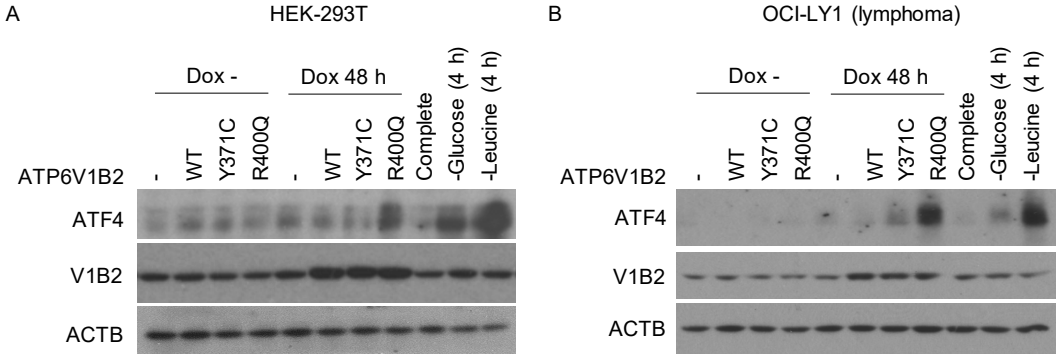
A
HEK-293T
Dox -
Dox 48 h
ATP6V1B2
-
WT
Y371C
R400Q
-
WT
Y371C
R400Q
Complete
-Glucose (4 h)
-Leucine (4 h)
ATF4
V1B2
ACTB
B
OCI-LY1 (lymphoma)
Dox -
Dox 48 h
ATP6V1B2
-
WT
Y371C
R400Q
-
WT
Y371C
R400Q
Complete
-Glucose (4 h)
-Leucine (4 h)
ATF4
V1B2
ACTB

S Figure 5

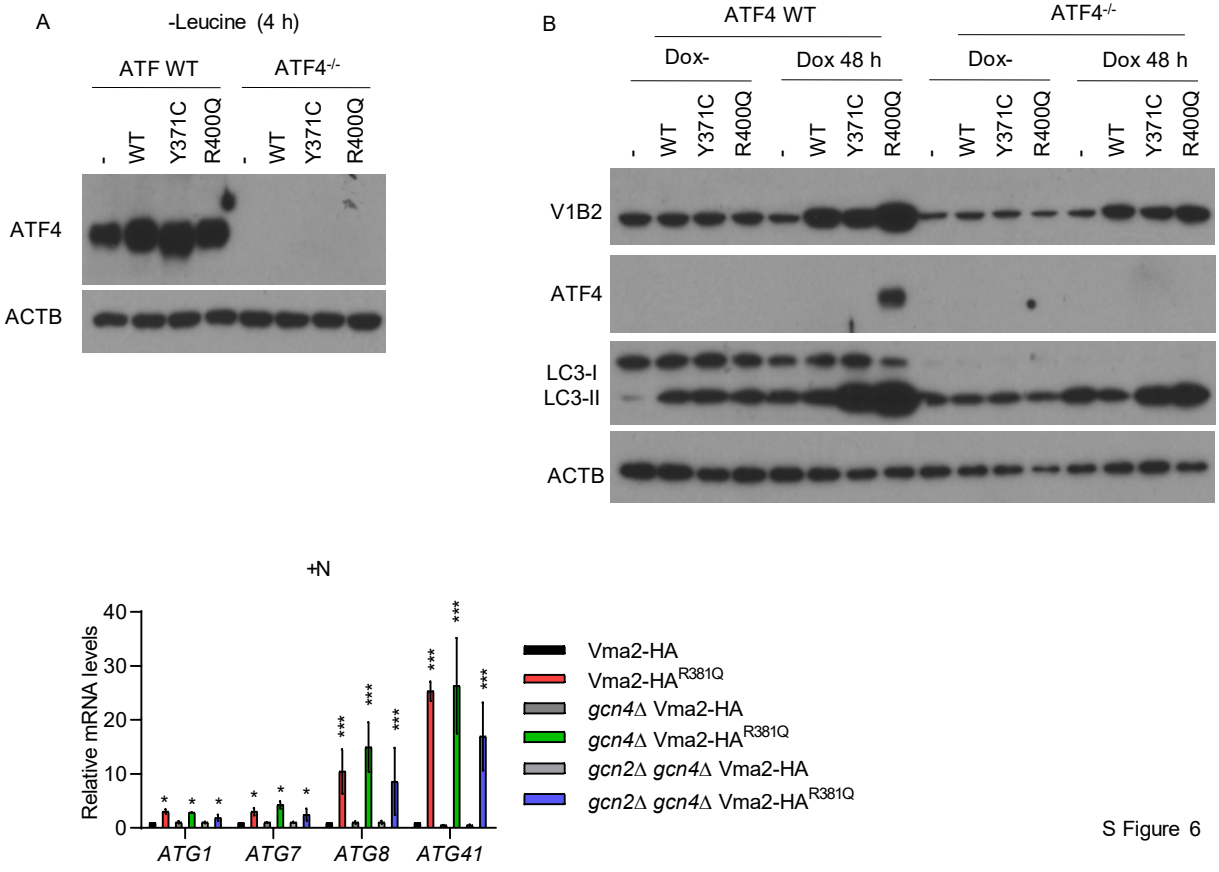
A
-Leucine (4 h)
ATF WT
ATF4-/-
-
WT
Y371C
R400Q
ATF4
ACTB
B
ATF4 WT
ATF4-/-
Dox-
Dox 48 h
V1B2
ATF4
LC3-I
LC3-II
ACTB
+N
Relative mRNA levels
ATG1
ATG7
ATG8
ATG41
Vma2-HA
Vma2-HA R381Q
gcn4Δ Vma2-HA
gcn4Δ Vma2-HA R381Q
gcn2Δ gcn4Δ Vma2-HA
gcn2Δ gcn4Δ Vma2-HA R381Q

S Figure 6

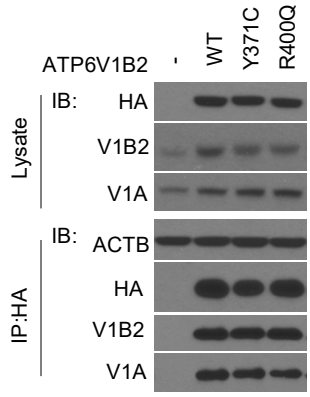
ATP6V1B2
-
WT
Y371C
R400Q
Lysate
IB:
HA
V1B2
V1A
IP:HA
IB:
ACTB
HA
V1B2
V1A

S Figure 7

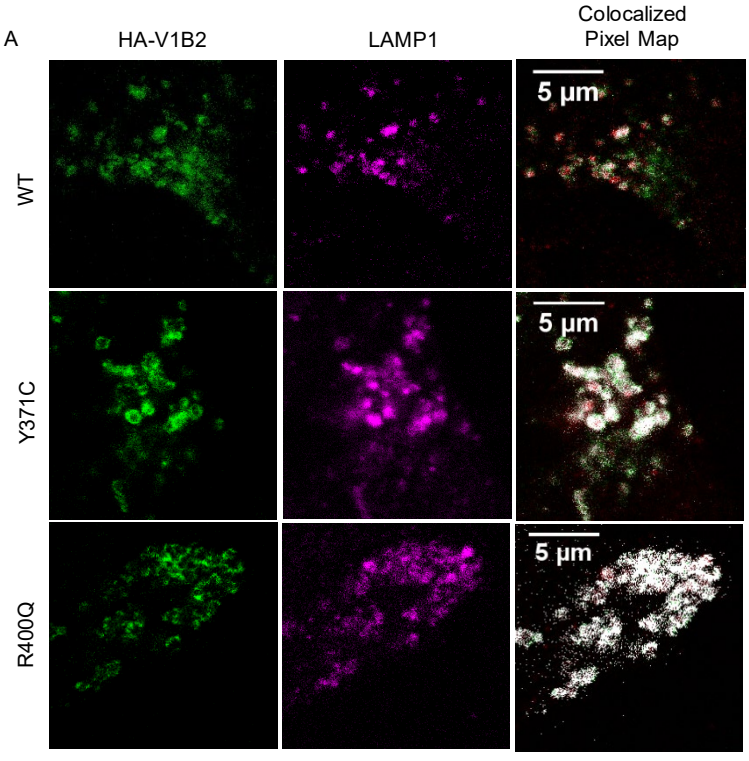
A
HA-V1B2
LAMP1
Colocalized Pixel Map
WT
Y371C
R400Q
5 μm
5 μm
5 μm

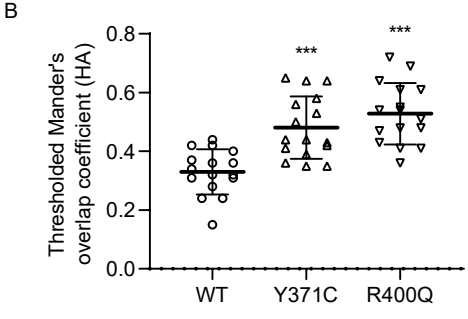
B
Thresholded Mander's overlap coefficient (HA)
0.8
0.6
0.4
0.2
0.0
***
***
WT
Y371C
R400Q

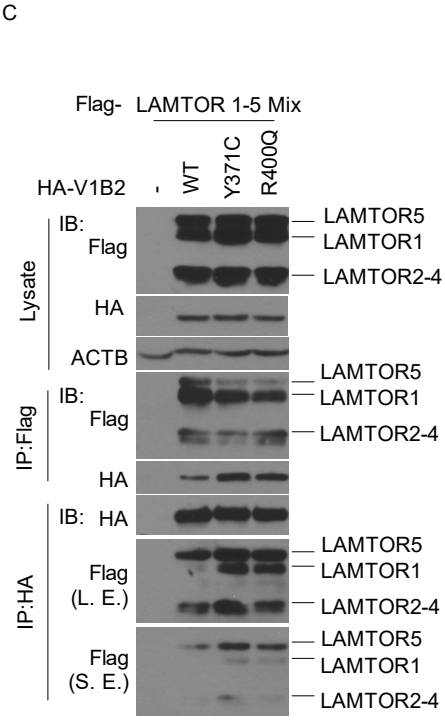
C
Flag-
LAMTOR 1-5 Mix
HA-V1B2
-
WT
Y371C
R400Q
Lysate
IB:
Flag
HA
ACTB
IP:Flag
IB:
Flag
HA
IP:HA
IB:
HA
Flag (L. E.)
Flag (S. E.)
LAMTOR5
LAMTOR1
LAMTOR2-4

S Figure 8

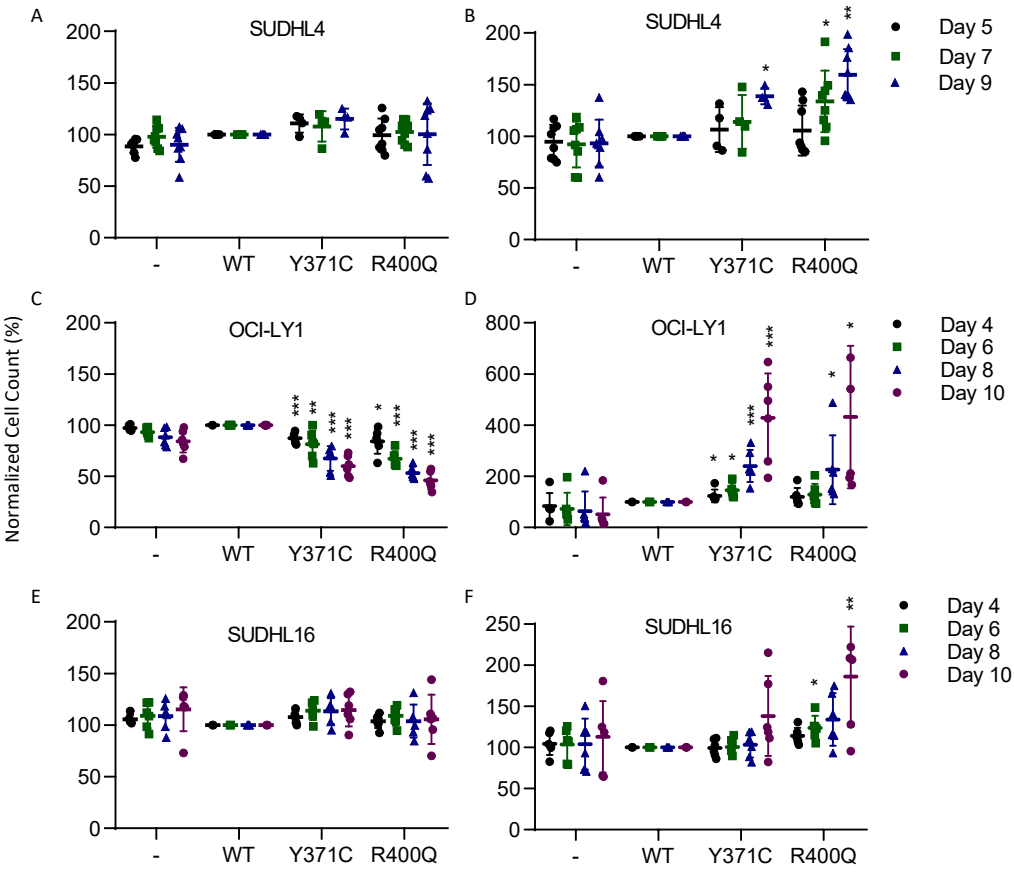
A
SUDHL4
200
150
100
50
0
-
WT
Y371C
R400Q
B
SUDHL4
Day 5
Day 7
Day 9
C
OCI-LY1
Normalized Cell Count (%)
D
OCI-LY1
800
600
400
200
Day 4
Day 6
Day 8
Day 10
E
SUDHL16
F
SUDHL16
250

S Figure 9

A

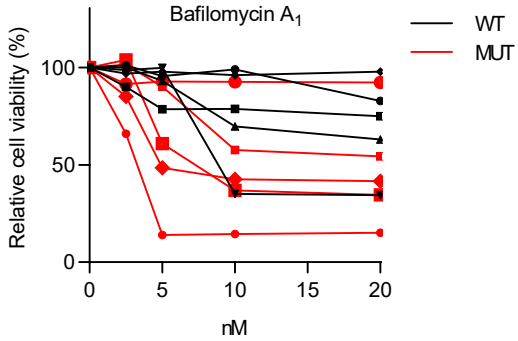

B

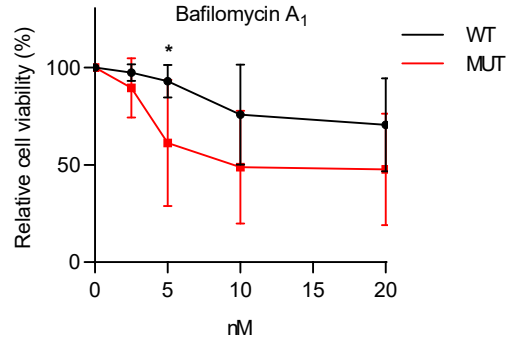

S Figure 10

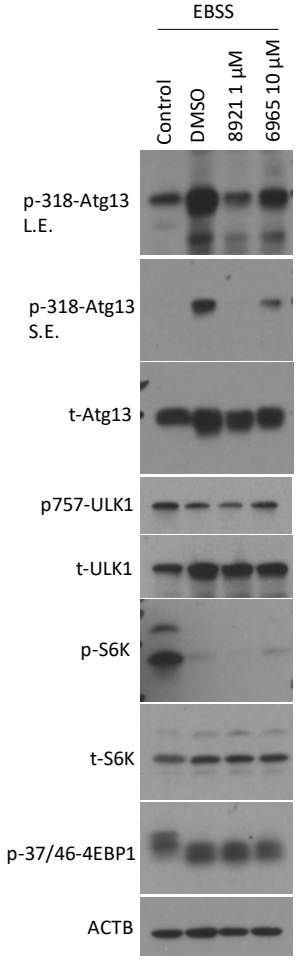
EBSS
Control
DMSO
8921 1 μM
6965 10 μM
p-318-Atg13 L.E.
p-318-Atg13 S.E.
t-Atg13
p757-ULK1
t-ULK1
p-S6K
t-S6K
p-37/46-4EBP1
ACTB

S Figure 11

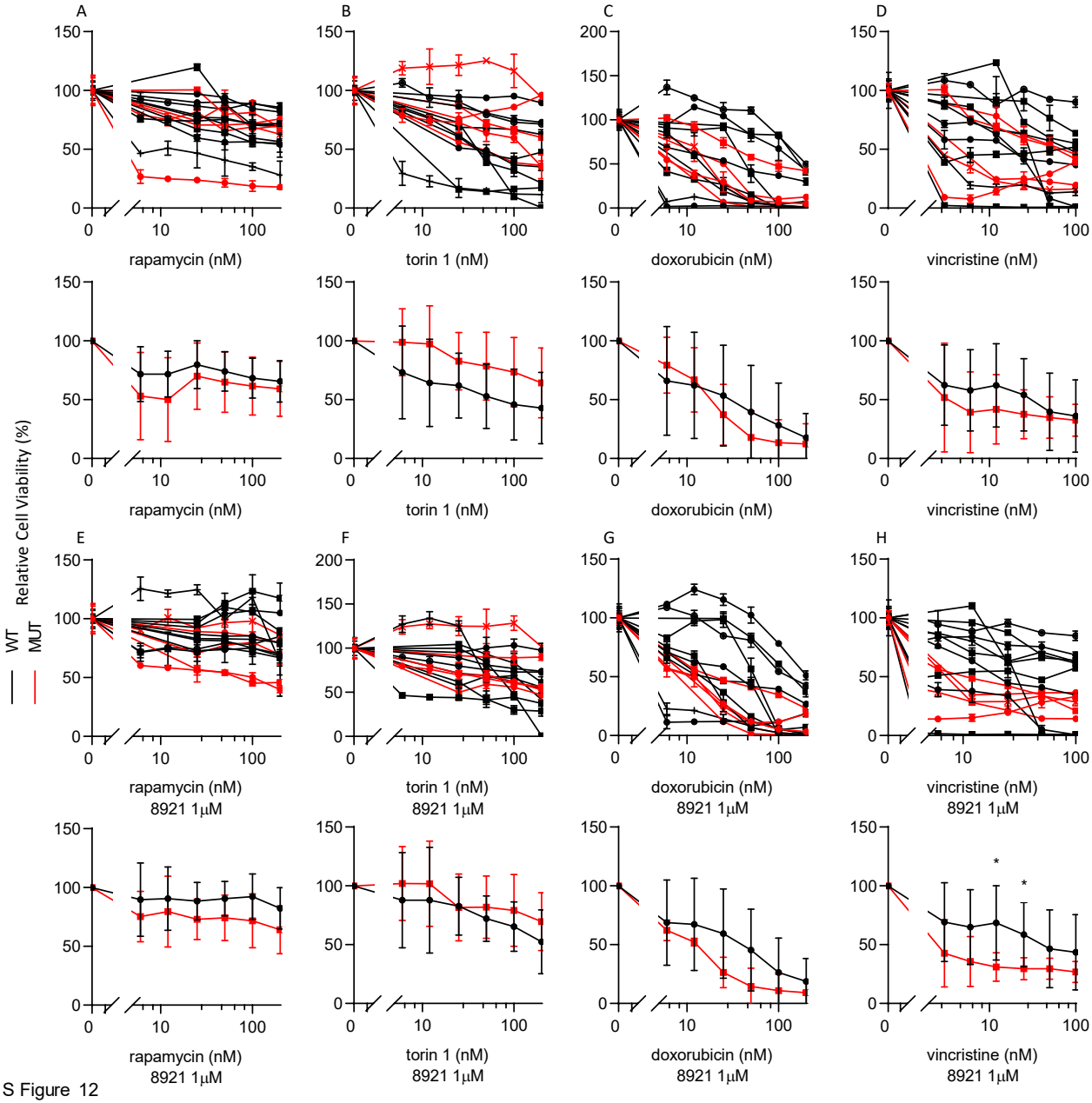
A
B
C
D
E
F
G
H
WT
MUT
Relative Cell Viability (%)
rapamycin (nM)
torin 1 (nM)
doxorubicin (nM)
vincristine (nM)
8921 1μM
*
*

S Figure 12

Supplemental Table 1. Antibodies used in this study.

Name	Company	Catalog #
anti-V1B2	Cell Signaling Technology	14488
anti-LC3A/B	Cell Signaling Technology	12741
anti-RPS6KB/S6 kinase	Cell Signaling Technology	9202
anti-p-RPS6KB/S6 kinase (Thr389)	Cell Signaling Technology	9205
anti-ATG7	Cell Signaling Technology	8558
anti-SQSTM1/p62	Cell Signaling Technology	5114
anti-ATF4	Cell Signaling Technology	11815
anti-p37/46-EIF4EBP1	Cell Signaling Technology	2855
anti-p65-EIF4EBP1	Cell Signaling Technology	9451
anti-p70-EIF4EBP1	Cell Signaling Technology	9455
anti-ULK1	Cell Signaling Technology	8054
anti-p757-ULK1	Cell Signaling Technology	6888
anti-p371-ULK1	Cell Signaling Technology	12753
anti-ATG13	Cell Signaling Technology	13273
anti-p-ATG13	Rockland	36708
anti-ACTB	Sigma-Aldrich	A544
anti-YFP	Clontech/TaKaRa	632381
anti-peroxidase (protein A)	Jackson Immunoresearch	323-005-024
goat anti-rabbit Alexa Fluor 488	Life Technologies	1790498
goat anti-mouse Alexa Fluor 647	Life Technologies	A21235

Follicular lymphoma-associated mutations in vacuolar ATPase ATP6V1B2 activate autophagic flux and MTOR

Fangyang Wang[1*], Damián Gatica[2,3*], Zhang Xiao Ying[1], Luke F. Peterson[1], Peter Kim[1], Denzil Bernard[1], Kamlai Saiya-Cork[1], Shaomeng Wang[1], Mark S. Kaminski[1], Alfred E. Chang[4], Tycel Phillips[1], Daniel J. Klionsky[2,3*] and Sami N. Malek[1,5*]

From the Department of Internal Medicine, Division of Hematology and Oncology[1], Life Sciences Institute[2], Department of Molecular, Cellular and Developmental Biology[3], Department of Surgery[4], University of Michigan, Ann Arbor, MI, USA.

SUPPLEMENTARY FIGURE AND TABLE LEGENDS

Supplementary Figure 1: A: Location of identified ATP6V1B2 mutation sites Y371C and R400Q (sticks) on homology models of V1B2 subunit of the vATPase. **B:** Conformational changes of yeast subunit B residues Y352 and R381 (shown as ball and sticks) in the 3 different yeast VMA2 catalytic states: open (subunit A: orange; subunit B: blue); loose (subunit A: yellow; subunit B: magenta) and tight (subunit A: grey; subunit B: pink). Residues of subunit A neighboring Y352 and R381 are shown as lines. Figures generated using Pymol.

Supplementary Figure 2: *S. Cerevisiae* strains carrying both WT and mutant R381Q Vma2-HA activate autophagic flux. To mimic the *ATP6V1B2* heterozygous mutation in mammalian cells, WT or R381Q *VMA2-HA* were integrated in the *S. cerevisiae* strain WLY176. Autophagy activity was measured under growing and nitrogen starvation conditions at the indicated timepoints using **A:** The Pho8Δ60 activity, and, **B:** The GFP-

Atg8 processing assay. Statistical comparison for SD-N (3h) conditions were done using t testing. * $p<0.05$.

Supplementary Figure 3: Phospho-4EBP1 measurements in inducible ATP6V1B2 mutant cell lines: A: Stable HEK293T cells were generated using the inducible lentiviral system pCW57.1 carrying either wild-type or mutated cDNAs encoding HA-tagged ATP6V1B2. Cells were induced with doxycycline 72 h and prepared for immunoblotting with various antibodies as indicated. Treatment with torin 1 at 50 nM for 4 h was used as control. One of three representative immunoblots is shown. **B-D:** Combined quantitation results from three independent experiments using ImageJ densitometry with results indexed to the measurements for empty vector with doxycycline induction. Statistical comparison for WT, Y371C and R400Q were done using t testing with Bonferroni corrections. * $p<0.05$. The mean and standard deviations are plotted. **B:** p70-4EBP1/t-4EBP1; **C:** p65-4EBP1/t-4EBP1; **D:** p37/46-4EBP1/t-4EBP1.

Supplementary Figure 4: Measurements of mTOR- and AMPK-dependent ULK1 phosphorylation in inducible ATP6V1B2 wild type and mutant cell lines: Inducible cell lines were left untreated (lanes 1-4) or treated with doxycycline for 48 h (lanes 5-8). Immunoblotting results for **A:** HEK293T cells and **B:** OCI-LY1 lymphoma cells. Protein lysates were prepared for immunoblotting with antibodies targeting epitopes as indicated. In parallel, cells were also grown in full medium, or glucose-free medium, or Leucine-free medium (lanes 9-11).

Supplementary Figure 5: Induction of ATF4 by ATP6V1B2 p. R400Q: Inducible cell lines were left untreated (lanes 1-4) or treated with doxycycline for 48 h (lanes 5-8). Immunoblotting results for **A:** HEK293T cells and **B:** OCI-LY1 lymphoma cells. Protein lysates were prepared for immunoblotting with antibodies targeting epitopes as indicated. In parallel, cells were also grown in full medium, or glucose-free medium, or Leucine-free medium (lanes 9-11).

Supplementary Figure 6: A: Generation of ATF4 null cells: ATF4 induction by leucine starvation (4h) in uninduced doxycycline-inducible HEK293T cells carrying empty vector or WT or mutated ATP6V1B2 parental (left) and *ATF4*$^{-/-}$ gene disrupted (using crispr-Cas9) cells (right). **B:** LC3-II levels in uninduced and induced doxycycline-inducible HEK293T cells carrying empty vector or WT or mutated ATP6V1B2 parental (left) cells and *ATF4*$^{-/-}$ gene disrupted (using crispr-Cas9) cells (right). **C: Induction of ATG genes by mutant Vma2^{R381Q}-HA:** *S. cerevisiae* strain WLY176 was used to generate *gcn2Δ*, gcn4*Δ* and *gcn2Δ*gcn4*Δ* deletion strains. Vma2-HA or mutant Vma2^{R381Q}-HA was knocked-in all three deletion strains. *ATG1, ATG7, ATG8 and ATG41* mRNA levels were determined by RT-qPCR. Error bars indicate the standard deviation of 3 independent experiments. ANOVA, *p< 0.05 ***p< 0.001.

Supplementary Figure 7: Results of co-immunoprecipitation of ATP6V1B2 and ATP6V1A. Immunoprecipitations were performed out of HEK293T cells transiently transfected with HA-tagged ATP6V1B2 wild type or mutants as indicated.

Supplementary Figure 8: Increased localization of follicular lymphoma-associated ATP6V1B2 mutant proteins to lysosomes. A: Stable HEK293T inducible cell lines carrying WT or mutated *ATP6V1B2* cDNAs were generated using the doxycycline-inducible lentiviral pCW57.1 vector. Following induction with doxycycline for 24 h, HEK293T cells were prepared for immunofluorescence staining with anti-HA and LAMP1 antibodies (LAMP1 is localized to the lysosomal membranes and is used as a colocalization marker). The colocalized pixel images and quantification were generated using ImageJ software. **B:** Mutated V1B2 proteins demonstrate increased colocalization with LAMP1 (image quantification). Colocalization was analyzed by Mander's overlap coefficient in ImageJ for 16 different regions in each group (N=16). Statistical comparison for WT, Y371C and R400Q were done using t testing with Bonferroni corrections. *** p<0.001. The mean and standard deviations are plotted. **C:** ATP6V1B2 mutants demonstrate modestly increased binding with LAMTOR1-LAMTOR5 (ragulator) components. HEK293T cell were transiently co-transfected as indicated with expression plasmids encoding Flag-tagged *LAMTOR1-LAMTOR5* cDNAs and either HA-tagged

ATP6V1B2 WT or the indicated ATP6V1B2 mutants. CHAPS detergent lysates were prepared and subjected to anti-HA-bead or anti-Flag-bead conjugate-mediated immunoprecipitations. Following washings, bound protein was eluted and fractioned by SDS-PAGE and prepared for immunoblotting with the indicated antibodies.

Supplementary Figure 9: Follicular lymphoma-associated ATP6V1B2 mutations increase the viability and growth of lymphoma cell lines under leucine starvation conditions. A-B: SUDHL4 cells were double spin-inoculated on day 0 and day 1 with bicistronic FG9 lentiviruses carrying WT or mutant *ATP6V1B2* cDNAs. The infection efficiency was confirmed on day 3 through FACS based on GFP fluorescence and was >90%. On day 3, cells were seeded at $5x10^5$ cells per ml and cultured in full RMPI 1640 medium supplemented with 10% FBS. Parallel cell aliquots were cultured under otherwise identical conditions but using only 25% of the leucine concentration. Cells were counted every other day using Trypan blue and diluted back to a concentration of $5x10^5$ cells per ml. The histograms were normalized to the counts for WT ATP6V1B2 indexed to 100% and are based on 4 independent experiments. **C-F:** Doxycycline-inducible stable OCI-LY1 or SUDHL16 cell lines were generated through infections with the pCW57.1 vector carrying WT or mutated *ATP6V1B2* cDNAs. After 48 h of doxycycline induction, cells were seeded at $5x10^5$ cells per ml and cultured in full RMPI 1640 medium supplemented with 10% FBS. Parallel cell aliquots were cultured under otherwise identical conditions but using only 25% of the leucine concentration. Cells were counted every other day using Trypan blue and diluted back to a concentration of $5x10^5$ cells per ml. The data were normalized to the counts for wild-type ATP6V1B2 indexed to 100% and are based on 3 independent experiments. Statistical comparison for WT, Y371C and R400Q were done using t testing with Bonferroni corrections. The mean and standard deviations are plotted. * $p< 0.05$, ** $p<0.01$, *** $p<0.001$.

Supplementary Figure 10: Follicular lymphoma-associated ATP6V1B2 mutations and dependence on autophagic flux for survival of primary FL B cells: A: Purified FL B cells carrying wild type (black; N=5) or mutant *ATP6V1B2* (red; N=4) were cultured in serum-supplemented RPMI1640 medium and treated with bafilomycin A_1 for 72 h at

the indicated concentrations. Cell viability was measured using ANXA5/annexin V-propidium iodide and is displayed normalized to the viability of cells cultured for 72 h but left untreated. **B:** composite of data shown in **panel A** with standard deviations (SD); Statistical comparison for each concentration were done using t testing. * $p<0.05$.

Supplementary Figure 11: Inhibition of ATG13 phosphorylation by chemical ULK1 inhibitors: HEK293T cells were cultured in EBSS buffer for 1 h alone, or in the presence of ULK1 kinase inhibitors at 1 μM MRT68921 (8921) or 10 μM SBI-0206965 (6965). Protein lysates were prepared for immunoblotting with antibodies targeting epitopes as indicated.

Supplementary Figure 12: Cell viability following drug treatment of primary purified human FL B cells: A-D: Purified human FL B cells harboring wild type or mutant *ATP6V1B2* were cultured in serum-supplemented RPMI 1640 medium containing 100% Leu and treated with rapamycin, torin 1, doxorubicin or vincristine for 72 h at the indicated concentrations. Cell viability was measured using Celltiter-Glo® and is displayed normalized to the viability of cells cultured for 72 h but left untreated. Red: mutant *ATP6V1B2*; Black: wild type *ATP6V1B2.* Upper row: data from individual FL samples; bottom row: mean plus standard deviations (SD) of data shown in the upper row. **E-H:** Purified human FL B cells harboring wild type or mutant *ATP6V1B2* were cultured in serum-supplemented RPMI 1640 medium containing 100% Leu and treated with rapamycin, torin 1, doxorubicin or vincristine combined with 1 μM of the ULK1 inhibitor MRT68921 for 72 h at the indicated concentrations. Cell viability was measured using Celltiter-Glo® and is displayed normalized to the viability of cells cultured for 72 h but left untreated. Red: mutant *ATP6V1B2*; Black: wild type *ATP6V1B2***.** Upper row: data from individual FL sample; bottom row: mean plus standard deviations (SD) of data shown in the upper row; Statistical comparisons for each concentration were done using t testing. * $p<0.05$.

Supplementary Table 1: Antibody sources